

---

# SAC: Accelerating and Structuring Self-Attention via Sparse Adaptive Connection

---

Xiaoya Li<sup>\*1</sup>, Yuxian Meng<sup>\*1</sup>, Qinghong Han<sup>1</sup>, Fei Wu<sup>2</sup> and Jiwei Li<sup>1</sup>

<sup>1</sup> Shannon.AI

<sup>2</sup> Computer Science Department, Zhejiang University

{xiaoya\_li, yuxian\_meng, qinghong\_han, jiwei\_li}@shannonai.com

## Abstract

While the self-attention mechanism has been widely used in a wide variety of tasks, it has the unfortunate property of a quadratic cost with respect to the input length, which makes it difficult to deal with long inputs. In this paper, we present a method for accelerating and structuring self-attentions: Sparse Adaptive Connection (SAC). In SAC, we regard the input sequence as a graph and attention operations are performed between linked nodes. In contrast with previous self-attention models with pre-defined structures (edges), the model learns to construct attention edges to improve task-specific performances. In this way, the model is able to select the most salient nodes and reduce the quadratic complexity regardless of the sequence length. Based on SAC, we show that previous variants of self-attention models are its special cases. Through extensive experiments on neural machine translation, language modeling, graph representation learning and image classification, we demonstrate SAC is competitive with state-of-the-art models while significantly reducing memory cost.<sup>1</sup>

## 1 Introduction

The self-attention mechanism has proved to benefit a wide range of fields and tasks, such as natural language processing (Vaswani et al., 2017), computer vision (Xu et al., 2015; Jaderberg et al., 2015; Bello et al., 2019; Parmar et al., 2019), video classification (Wang et al., 2018) and graph modeling (Veličković et al., 2018; Lee et al., 2019). The attention mechanism allows the model to attend to different parts of the input and capture the most salient features, and provides with the ability to handle dependencies between elements across long distances (Dai et al., 2019).

Two conspicuous problems stand out with the self-attention mechanism: (1) the memory complexity is quadratic with respect to the input length, making it infeasible to handle long sequences; and (2) the self-attention operations are performed in a pre-defined structure (usually fully-connected), which not only is costly but also lacks for the ability to learn the optimal attention structure optimized for the performance in the downstream tasks Child et al. (2019); Sukhbaatar et al. (2019). These observations indicate that the fully-connected structure for self-attention operations can be replaced by a more sparse one where only specific edges are constructed for attention operations.

In this paper, we present Sparse Adaptive Connection (SAC), which replaces the fully-connected structure in self-attention with a sparse graph-like structure adapted to different tasks. In SAC, we regard the input as a graph where a node could be a token in the sequence or a flattened feature map of an image, and an edge between a pair of nodes represents they can attend to each other. To select edges, we propose an Edge Predictor which utilizes an LSTM model to dynamically predict pairs of nodes that represent two ends of an edge. In contrast with previous self-attention models with pre-defined attention structures (edges), SAC learns to construct attention edges adaptively,

---

<sup>1</sup>Xiaoya and Yuxian contributed equally to this paper.

which are optimized to improve task-specific performances using reinforcement learning models. We evaluate the proposed model on four tasks: neural machine translation, language modeling, graph representation learning and image classification, and demonstrate that SAC learns to select the most salient nodes to attend to each other and is free from heavy memory cost while achieving strong performances.

## 2 Related Work

### 2.1 Modifying Self-Attention in Transformer

Many recent researches have focused on modifying the structure of self-attention to relieve the computation and memory burden. Transformer-XL (Dai et al., 2019) enables learning long-term dependency by introducing a segment-level recurrence mechanism and a novel relative position encoding scheme. (Guo et al., 2019) proposed Star Transformer, a variant of Transformer which replaces the fully-connected structure in self-attention with a star-shaped topology, where all tokens are connected with a relay node. (Child et al., 2019; Kitaev et al., 2020) suggest sparsifying Transformer by focusing only on a fraction of attention connections. (Child et al., 2019) introduced sparse factorizations of the attention matrix, which scale as  $O(n\sqrt[n]{n})$  with the sequence length, and a set of sparse attention kernels which efficiently compute subsets of the attention matrix. (Kitaev et al., 2020) proposed Reformer, a more efficient yet complicated method for computing self-attention, where the dot-product attention is replaced by one that uses a locality-sensitive hashing, reducing the complexity from  $O(n^2)$  to  $O(n \log n)$ . (Ye et al., 2019) partitioned the sequence to different multi-scale spans and attended the context information from fine-grain to coarse-grain as the relative distance increases. All above works rely on manually designed structures. Our work is inspired by (Sukhbaatar et al., 2019), which takes a step forward and uses a novel adaptive self-attention mechanism that can learn its optimal attention span for each head.

### 2.2 Applying Attention over Graphs

Graph neural networks (GNNs) are known at learning local contextual information by encoding attribute features (Kipf and Welling, 2016; Hamilton et al., 2017c), but they are not able to explicitly distinguish the most salient nodes from all its neighbors, neither can they directly attend to the nodes that are beyond one-hop away. Much work has investigated the effect of attention on GNNs (Veličković et al., 2018; Abu-El-Haija et al., 2018; Lee et al., 2018; Veličković et al., 2019). (Veličković et al., 2018) extended self-attention to graphs by enabling each node to attend over its neighbors, achieving state-of-the-art results for semi-supervised node classification tasks. But they simply applied self-attention over graphs to all neighbors of a node, which might be a problem when dealing with large and noisy graphs where only few neighbors need to be aggregated. (Ye and Ji, 2019) proposed Sparse Graph Attention Network which uses a binary gate to control whether each edge should be engaged. However, these works lack the ability to aggregate long-range dependencies in graphs, that is, they only consider neighbors that are one hop away, for which various methods have been proposed to tackle this issue (Ye et al., 2020; Zhang et al., 2020; Pei et al., 2020). Similar to graphs, (Bello et al., 2019) introduced a novel two-dimensional relative self-attention mechanism for images and augmented convolutional operators with this self-attention method, showing systematic improvements on both image classification and object detection tasks across a wide range of architectures.

## 3 Background

### 3.1 Graph Convolutional Networks

Graph Convolutional Networks (GCNs) are a kind of neural networks that operate on graph structures (Kipf and Welling, 2016). Given a graph with  $L$  nodes  $\{e_1, \dots, e_L\}$  and an  $L \times L$  adjacency matrix  $\mathbf{A}$  where  $\mathbf{A}_{ij} = \mathbf{A}_{ji} = 1$  means there is an undirected edge between node  $e_i$  and node  $e_j$ , otherwise  $\mathbf{A}_{ij} = \mathbf{A}_{ji} = 0$ , we compute the hidden representation  $\mathbf{h}_i^n$  of node  $e_i$  in the  $n$ -th layer, for which

GCNs aggregate all representations of its neighboring nodes in the previous layer:

$$\mathbf{h}_i^n = \rho \left( \sum_{j=1}^L \mathbf{A}_{ij} \mathbf{W}^n \mathbf{h}_j^{n-1} + \mathbf{b}^n \right) \quad (1)$$

where  $\mathbf{W}^n, \mathbf{b}^n$  are learnable parameters, and  $\rho$  is an activation function. We use  $\rho = \text{ReLU}$  in this work.  $\mathbf{h}_i^0 = \mathbf{w}_i$  is the initial node representation of node  $i$ . In the following of this paper, we use  $\mathcal{N}(e_i)$  to denote the set of all neighbors of  $e_i$ .

### 3.2 Multi-Head Self-Attention

Given a set of nodes<sup>2</sup>  $\{e_1, \dots, e_L\}$  as inputs, self-attention iteratively computes the representation of  $e_i$  in the  $n$ -th layer by attending to all its neighbors  $\mathcal{N}(e_i)$ , which is defined as follows:

$$\begin{aligned} \tilde{\mathbf{h}}_i^n &= \sum_{e_j \in \mathcal{N}(e_i)} \alpha_{ij} \mathbf{v}_j^{n-1}, \quad \alpha_{ij} = \text{softmax} \left( \frac{(\mathbf{q}_i^{n-1})^\top \mathbf{k}_j^{n-1}}{\sqrt{d}} \right) \\ \text{and} \quad \mathbf{q}_i^{n-1} &= \mathbf{W}^Q \mathbf{h}_i^{n-1}, \quad \mathbf{k}_j^{n-1} = \mathbf{W}^K \mathbf{h}_j^{n-1}, \quad \mathbf{v}_j^{n-1} = \mathbf{W}^V \mathbf{h}_j^{n-1} \end{aligned} \quad (2)$$

where  $d$  is the hidden dimension,  $\mathbf{W}^Q, \mathbf{W}^K, \mathbf{W}^V$  are learnable parameters and  $\mathbf{q}, \mathbf{k}, \mathbf{v}$  correspond to queries, keys and values, respectively. The multi-head mechanism linearly projects the queries, keys and values multiple times with different learned linear projections, and then performs self-attention in parallel, after which the results are concatenated and again projected:

$$\mathbf{h}_i^n = \text{Concat}(\tilde{\mathbf{h}}_i^{n,1}, \dots, \tilde{\mathbf{h}}_i^{n,m}) \mathbf{W}^O \quad (3)$$

where the superscript  $1, \dots, m$  denotes the head number, and  $\mathbf{W}^O$  is learnable parameters. After  $N$  iterations, we obtain the final representation for each node  $\mathbf{h}_i^N$ .

## 4 Sparse Adaptive Connection for Self-Attention

The key point in SAC is to use an LSTM edge predictor to predict edges for self-attention operations between nodes, where a node could be a token in the sequence or an flattened feature map of an image. Self-attention operations are performed between linked nodes instead of in a fully-connected manner. The LSTM edge predictor is optimized to improve task-specific performances using reinforcement learning models.

### 4.1 LSTM Edge Predictor

In SAC, an edge predictor is used to construct edges between nodes for self-attention operations. Suppose that we are given a set of nodes  $\{e_1, \dots, e_L\}$  with no edge between any pair of nodes when initialization, our aim is to generate edges using this edge predictor, with the total number  $\alpha L$  for each layer, where  $\alpha$  is a hyperparameter deciding how many edges should be constructed for each node on average. The Edge Predictor uses an LSTM model (Hochreiter and Schmidhuber, 1997) as a backbone and sequentially predicts edges. The prediction of an edge is decoupled into the prediction of the original node and the destination node pair.

More formally, the input to Edge Predictor is a special token “[SOS]”, and the model proceeds to predict the original node and destination node of all edges ( $2\alpha L$  nodes in total) for the first layer, denoted by  $\{y_1^1, y_2^1, \dots, y_{2\alpha L}^1\}$ , where the superscript denoted the index of the layer and the subscript denoted the index of the predicted node. At each time step, the input to the LSTM model is the representation  $\mathbf{h}_{y_t}$  for the node that has just been predicted. Then it is combined with the representation previously constructed representation  $\mathbf{g}_t$  to obtain  $\mathbf{g}_{t+1}$  representing the current time-step using LSTMs, and  $\mathbf{g}_{t+1}$  is used to predict the following node using the softmax function. The projection matrix before softmax  $\mathbf{W}$  shares embeddings with node representations, where each

<sup>2</sup>We use the term “node” in a broad sense of denoting any particular unit in text, images or graphs.

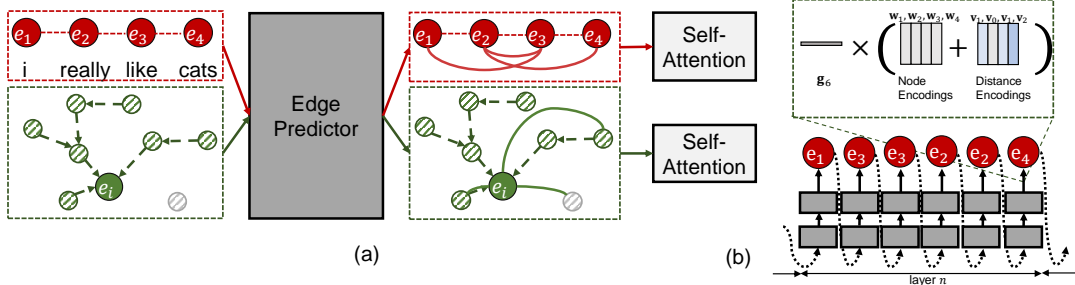


Figure 1: An illustration of the proposed Sparse Adaptive Connection. (a) shows the process of SAC to construct edges and then perform self-attention on these edges (Red is for text and green is for graphs). (b) shows the edge prediction process of (a, red) with distance encodings.

column  $w_i$  is the vector representation for node  $e_i$ . The probability of predicting node  $y_{t+1}$  given  $g_{t+1}$  is thus given by:

$$p(y_{t+1} = e_i) = \frac{\exp(g_{t+1}^T \cdot w_i)}{\sum_j \exp(g_{t+1}^T \cdot w_j)} \quad (4)$$

This process is repeated  $2\alpha L$  times. After the end of  $\alpha L$  edge predictions, we update the representation for each node based on self-attention as will be detailed in Section 4.1 for different tasks, and proceed to the next layer. For node predictions in the following layer, the initial input now becomes hidden state for the last time-step of the previous layer. The entire process is repeated  $N$  times, where  $N$  denotes the number of self-attention layers and the resulted nodes in layer  $n$  are  $\{y_1^n, y_2^n, \dots, y_{2\alpha L}^n\}$ . Compared to separately predicting edges for each node, this approach is more flexible and gives us finer control of the total number of edges we would like to construct. More importantly, this process is aware of previous constructed edges, both in the current layer and previous layers. The recurrent edge predictor is shown in Figure 1(b). We implement it using a single-layer LSTM model.

The vanilla version of the Edge Predictor can be further regulated (and also simplified) with prior knowledge for preferable graph structures. For example, to reduce the computational cost, we can enforce the edge structure to be the same for all layers, where the process is only executed once instead of  $N$  times; As another example, to enforce each node to be connected in each layer, for each node  $e_i$ , it is repeatedly fed to the predictor  $\alpha$  times as the original node, and we only predict the destination node. The graph can be either directed graph or undirected graph, depending on how we want self-attention to be computed.

Once having constructed all edges for each layer, we can immediately obtain the set of neighbors  $\mathcal{N}(e_i^n)$  for each node  $e_i$  in the  $n^{th}$  layer. Self-attention operations with multi-head mechanism are then performed on its neighbors for each node. For text tasks, we regard each token as a node. For graph-like structures, we treat nodes in the original graph as nodes. For images, the input  $(H, W, F_{in})$  dimensional sensor is reshaped to a  $HW \times F_{in}$  matrix, where each row can be thought as a node by our definition.

## 4.2 Distance Encoding

The input graph intrinsically displays some degree of structures. For example, in a sequence of natural language tokens, the relative distance between two tokens in the sequence or the corresponding parse tree encodes structural information. As another example, in the task of node representation learning in graphs (Yang et al., 2016b; Veličković et al., 2017; Xu et al., 2018), the graph originally comes with the node edges. The LSTM edge predictor described above ignores this structure. To leverage original structural information, we propose distance encodings to incorporate graph structure into the edge predictor. Distance encodings only affect the destination node predictions. In contrast to only using node embedding matrix  $\mathbf{W}$ , we add an extra *distance matrix*  $\mathbf{V}$  that encodes distance information to the original projection matrix  $\mathbf{W}$ , giving  $\mathbf{V} + \mathbf{W}$ . Each column in  $\mathbf{V}$  is its corresponding distance representation to the original node.

For example in Figure 1, at time-step 6, when two edges  $(e_1, e_3), (e_3, e_2)$ , and one origin node  $e_2$  have been generated, we are to use  $g_5 \in \mathbb{R}^d$ , the output of the LSTM model at time-step 5, to predict

the node at time-step 6. According to the original structure, the distance between  $e_2$  (the current origin node) and all the nodes  $e_1, e_2, e_3, e_4$  are 1,0,1, 2 respectively. The distance vectors are thus  $\mathbf{v}_1, \mathbf{v}_0, \mathbf{v}_1, \mathbf{v}_2$ , which are vectors of size  $\mathbb{R}^d$  to be learned. and make up the distance encoding matrix  $\mathbf{V} \in \mathbb{R}^{d \times L}$ . Intuitively, this process also discourages generating duplicate edges and leverages the original structural information.

In contrast to Veličković et al. (2017) where attention operations are only performed between nodes with literal edges in the original graph, SAC offers the flexibility in leveraging the original graph structure and influence from the training signals. Additionally, SAC allows for more convenient information exchange between similar nodes that are far away in terms of distance in the original graph structure, which is because the connection construction stage has the ability to connect any pair nodes in the graph. This ability potentially leads to better performances.

### 4.3 Training

Directly training the edge predictor is impractical since we have no access to the ground-truth edges. We use REINFORCE (Williams, 1992), which is an instance of a broader class of policy gradient methods for optimization. The main idea is to use reinforcement learning to discover the best edge connections for self-attention operations.

Each action  $a$  is the node predicted by edge predictor. Let  $\Theta$  denote parameters of the edge predictor and  $\Phi$  denote the parameters of the main network which maps an input to its final label based on a pre-defined self-attention structure. Under the framework of reinforcement learning, we ask the edge predictor to maximize its reward  $R(\Theta)$ , which is the log probability of predicting the correct label, e.g., for neural machine translation the reward  $R$  is the average log probability of golden target tokens; for image classification, the reward the log probability of the correct label. Consider the simple case where different attention layers use the same node connections, by sampling a sequence of nodes from the edge predictor, we are able to update the parameters in edge predictor using policy gradients:

$$\nabla_{\theta} J(\Theta) = \sum_{i=1}^{2\alpha L} \nabla_{\Theta} \log p(a_i | a_{1:i-1}; \Theta) (R(\Theta) - b) \quad (5)$$

where  $b$  denotes the baseline which is the average of the previous rewards.  $\Phi$  is updated directly based on the log-likelihood.

### 4.4 Connection to Existing Methods

In this subsection, we describe the connection between SAC and previous variants of self-attentions, and show that these variants computing self-attention are special cases of SAC if we slightly modify the edge predictor. For ease of exposition, we use  $\text{EP}(\mathbf{e}) = \{(e_i, e_j)\}$  to denote the collection of all edges for self-attention operations.

**Connection to vanilla self-attention (Vaswani et al., 2017)** The vanilla self-attention links each pair of nodes, where  $\text{EP}(\mathbf{e})$  can be described as  $\text{EP}(\mathbf{e}) = \{(e_i, e_j) | i \in [1, L]\}$ .

**Connection to Transformer-XL (Dai et al., 2019)** Transformer-XL treats the text in a segment-by-segment style. Self-attention operations are performed between nodes within the same segment.  $\text{EP}(\mathbf{e})$  can be described as  $\text{EP}(\mathbf{e}) = \{(e_i, e_j) | i \in [1, L]; j \in \text{Segment}(i)\}$ .

**Connection to Adaptive Span Transformer (Sukhbaatar et al., 2019)** Adaptive Span Transformer learns an optimal attention span for each head. Suppose the span size assigned to head  $t$  is  $s$ , then  $\text{EP}(\mathbf{e}, \mathbf{t})$  can be described by:  $\text{EP}(\mathbf{e}) = \{(e_i, e_j) | i \in [1, L]; j = i, i-1, \dots, i-s+1; \text{span} = t\}$ .

**Connection to BP-Transformer (Ye et al., 2019)** BP-Transformer constructed a tree-like graph by adding span nodes apart from token nodes. There are  $2L - 1$  nodes in total, where  $L$  is the sequence length. In BP-Transformer, each token (leaf) node attends to each span (non-leaf) node that includes it, which we refer to as  $\text{Ancestor}(e_i)$  for node  $e_i$ . It is easy to prove that a leaf node is associated with  $\lfloor \log_2 L \rfloor$  non-leaf nodes (and thus attends to  $\lfloor \log_2 L \rfloor$  nodes). Therefore, we have  $\text{EP}(\mathbf{e}) = \{(e_i, e_j) | i \in [1, L]; j \in \text{Ancestor}(e_i)\}$ .

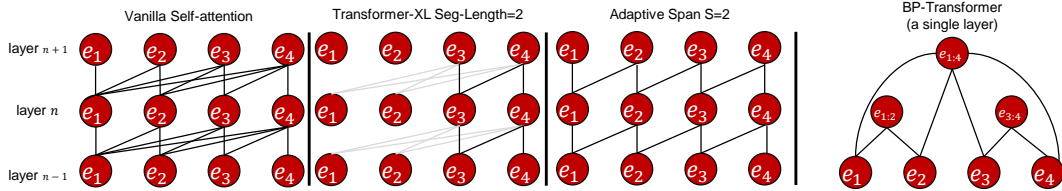


Figure 2: Connection of SAC to other methods for computing self-attention.

Model	H (heads)	N (blocks)	edges	dev	test
Transformer Base (Vaswani et al., 2017)	8	6	$L^2$	25.8	27.3
BP base (Ye et al., 2019)					27.6
Reversible base (Kitaev et al., 2020)					28.1
SAC base	8	6	$2L$	17.4	18.3
SAC base	8	6	$5L$	25.6	27.0
SAC base	8	6	$10L$	26.0	27.7
SAC base	8	6	$15L$	25.6	27.4
SAC base	16	6	$10L$	26.2	28.0
SAC base	16	12	$10L$	26.4	<b>28.2</b>
Transformer big (Vaswani et al., 2017)	16	6	$L^2$	26.4	28.4
Reversible big (Kitaev et al., 2020)					29.1
SAC Large	16	6	$10L$	26.7	28.9
SAC Large	16	18	$10L$	26.9	29.4
SAC Large (dependency)	16	18	$10L$	26.9	<b>29.5</b>

Table 1: BLEU scores on the newstest2013 for development and newstest2014 for test for WMT English-German.  $L$  denotes the length of the input sequence.

## 5 Experiments

We experiment the proposed model on the following four tasks, neural machine translation, language modeling, node representation learning in graphs, and image classification.

### 5.1 Machine Translation

We use the encoder-decoder model (Bahdanau et al., 2014; Vaswani et al., 2017) as the backbone for machine translation. For the encoder, SAC constructs  $\alpha L$  edges for each layer and self-attention operations are performed between connected nodes. For the decoder, masked attention (Vaswani et al., 2017) is applied. Specifically, given a newly generated target node, it can attend to all source nodes, dummy nodes, target nodes that come beforehand, but not target nodes that come afterwards. We again use SAC to construct edges between the newly generated node and the preceding nodes, where the input node to the edge predictor is forced to be the newly generated node, and the output node is limited to preceding nodes and the dummy nodes.

Following Vaswani et al. (2017); Ott et al. (2018); Kitaev et al. (2020), we used the standard WMT 2014 English-German dataset to test the proposed model. The dataset consists of about 4.5 million sentence pairs. Sentences are encoded using BPE (Sennrich et al., 2016), which has a shared source target vocabulary of about 37000 tokens. For fair comparison, we used the Adam optimizer (Kingma and Ba, 2014) with  $\beta_1 = 0.9$ ,  $\beta_2 = 0.98$  and  $\epsilon = 10^{-9}$  for all models. Label smoothing (Szegedy et al., 2016) with  $\epsilon = 0.1$  is applied for all models. For the base setup, following Vaswani et al. (2017), the dimensionality of inputs and outputs  $d_{\text{model}}$  is set to 512, and the inner-layer has dimensionality  $d_{\text{ff}}$  is set to 2,048. For big models,  $d_{\text{model}}$  is set to 1,024 and  $d_{\text{ff}}$  is set to 4,096. Models are run on 8 NVIDIA V100 GPUs.

Results are shown in Table 1. As we gradually increase the number of edges for each layer (from 2 to 5 to 10 to 20 per node), we can see that the performance first increases, reaching the highest with  $\alpha$  set to 10, and then decreases. This means that performing attention operations between all pairs is not only unnecessary, but can hurt the performance. Memory saved from sparse connections

Method	Enwiki8	Text8	Params
Trans(AI-Rfou et al., 2019)	1.11	1.18	44M
Trans-XL (Dai et al., 2019)	1.06	-	41M
Adaptive(Sukhbaatar et al., 2019)	1.02	1.11	39M
BPT (Ye et al., 2019)	1.02	1.11	38M
SAC (8 heads, 12 blocks)	1.02	1.07	39M

Table 2: Performances on language modeling datasets.

allow for more heads to perform attentions and deeper networks with more blocks, leading to better performances over vanilla transformers. We also implement a dependency-based model, in which English sources were first parsed using Stanford Dependency parser (Chen and Manning, 2014). Relative positions between nodes in the dependency trees are encoded in distance encodings of the edge predictor. The introduction of dependency parser for attention construction introduces +0.14 BLEU score boost.

## 5.2 Language Modeling

We use character-level language modeling datasets to evaluate SAC’s ability to handle long-term dependencies. We use Enwiki8 (Mahoney, 2011) and Text8 (Mahoney, 2011) for evaluation and report the values of BPC for different models. We use the Transformer decoder architecture as the backbone. We compare SAC with other variations of transformers to fit long sequences into the model, including the vanilla Transformer (AI-Rfou et al., 2019), which splits the whole sequence into smaller segments, and only trains the model within each segment and ignore the rest; Transformer-XL (Sukhbaatar et al., 2019) that adopts a recurrence mechanism to cache the memory of previous segments; adaptive span model (Sukhbaatar et al., 2019) that assigns different heads with different text spans in an adaptive fashion; and the BP-Transformer (Ye et al., 2019) that splits the sequence using binary trees. For SAC,  $\alpha$  is set to 256 for each node. The relatively small memory cost allows the model to look at a maximum context of 50k characters. Input dimensionality is set to 512, and the inner-layer has dimensionality 2,048. Following (Sukhbaatar et al., 2019) We use Adagrad for optimization, with a batch size of 64 and fixed learning rate of 0.07 and 32k warm-up steps. We use a block of 512 consecutive characters and compute the loss and gradient for each of those 512 characters.

Results are shown in Table2. As can be seen, SAC outperforms the other Transformers by 0.04 bcp on Text8 while significantly reducing the memory usage for large attention spans. For Enwiki8, it ties with the best BPT model, achieving 1.02 bcp score. The improvement validates the importance modeling long-term dependencies with limited available memory.

## 5.3 Representation Learning in Graphs

We test the performance of the proposed model on both transductive and inductive benchmark datasets for representation learning in graphs in a semi-supervised setting. For the transductive setup, we used the three standard citation network benchmarks, Cora, Citeseer and Pubmed (Sen et al., 2008). We followed the transductive setup adopted in (Yang et al., 2016b; Veličković et al., 2017; Xu et al., 2018), where nodes correspond to documents and edges to (undirected) citations. In the transductive setup, the training algorithm has access to all of the nodes’ feature vectors and labels, and predictions are performed on the test nodes. Cora contains 2708 nodes, 5429 edges, 7 classes and 1433 features per node. Citeseer contains 3327 nodes, 4732 edges, 6 classes and 3703 features per node. Pubmed contains 19717 nodes, 44338 edges, 3 classes and 500 features per node. For the inductive setup, we used the Protein-protein interaction dataset (PPI) (Zitnik and Leskovec, 2017), which aims at classifying protein roles such as cellular functions and gene ontology in various protein-protein interaction (PPI) graphs, where each graph corresponds to a different human tissue. Critically, testing graphs remain completely unobserved during training. The dataset has 56.9K nodes, 806.2 edges with 121 classes. The average number of nodes per graph is 2372. Each node has 50 features that are composed of positional gene sets, motif gene sets and immunological signatures. To construct the graphs, we used the preprocessed data provided by Hamilton et al. (2017a). The average number of nodes per graph is 2372. Each node has 50 features that are composed of positional gene sets, motif gene sets and immunological signatures. There are 121 labels for each node set from gene

Available data	Method	Cora	Citeseer	Pubmed	PPI
A	DeepWalk (Perozzi et al., 2014)	67.2	43.2	65.3	–
X, A	DGI (Veličković et al., 2019)	82.3	71.8	76.8	63.8
X, A	GraphSAGE (Hamilton et al., 2017b)	–	–	–	50.2
A, Y	LP (Zhu et al., 2003)	68.0	45.3	63.0	–
A, Y	ICA (Lu and Getoor, 2003)	75.1	69.1	73.9	–
X, A, Y	ManiReg (Belkin et al., 2006)	59.5	60.1	70.7	–
X, A, Y	SemiEmb (Weston et al., 2012)	59.0	59.6	71.7	–
X, A, Y	Planetoid (Yang et al., 2016a)	75.7	64.7	77.2	–
X, A, Y	Chebyshev (Defferrard et al., 2016)	81.2	69.8	74.4	–
X, A, Y	GCN (Kipf and Welling, 2016)	81.5	70.3	70.0	–
X, A, Y	MoNet (Monti et al., 2017)	81.7	–	78.8	–
X, A, Y	SGC (Wu et al., 2019)	81.0	71.9	78.9	–
X, A, Y	AdaLNet (Liao et al., 2019)	80.4	68.7	78.1	–
X, A, Y	SGAT (Ye and Ji, 2019)	84.2	68.2	77.6	96.6
X, A, Y	CurvGN-n (Ye et al., 2020)	82.7	72.1	79.2	–
X, A, Y	GAT (Veličković et al., 2017)	83.0	72.5	79.0	97.3
X, A, Y	SAC	<b>84.8</b>	<b>73.8</b>	<b>79.7</b>	<b>98.4</b>

Table 3: Summary of results in terms of classification accuracies on transductive tasks (Cora, Citeseer and Pubmed) or micro-averaged F1 score on inductive tasks (PPI). In the first column, we report the kind of data available to each method during training (X: features, A adjacency matrix, Y: labels).

ontology, collected from the Molecular Signatures Database (Liberzon et al., 2011), and a node can have several labels simultaneously.

The difference between SAC and (Veličković et al., 2017) is that the latter performs self-attention operations between nodes that are connected through graph edges, while SAC performs self-attention operations between nodes linked by the edge predictor. For fast convergence, we initialize SAC using the pretrained attention model (Veličković et al., 2017), where attention links are just edges in the original graph. Then we start exploring edge construction across all nodes. The number of attention heads is fixed to 8 and the number of blocks is set to 12. We experiment with different values of  $\alpha$ , i.e. [5, 10, 50, 100] unless the memory usage reaches limitation.

We train all models with Adam (Kingma and Ba, 2014) and early stopping on the validation set. The initial learning rate is treated as a hyper-parameter trained on the validation set. Following (Veličković et al., 2017), we run 100 epochs in total and use an early stopping strategy on both the cross-entropy loss and accuracy for transductive tasks and micro-F1 for inductive tasks. Each experiment is repeated three times and we report the mean value.

Results are shown in Table 3. We note that SAC achieves significant performance boosts over existing methods across all four datasets, i.e., outperforms our implemented GAT +1.8, +1.1, +0.7 and +1.1 respectively on Cora, Citeseer, Pubmed and PPI. The explanation for SAC’s advantage is as follows: graph node representation learning concerns about both label propagation and relatedness between nearby nodes in the vector space, the latter of which is what GCN handles. As verified in many recent works Liu et al. (2018); Wang and Leskovec (2020), combining both facets leads to better performances. The attention edge prediction stage in SAC fosters information exchange between nodes that are not directly linked in graph but similar in terms of label propagation. SAC actually offers the probability in bridging the aspects, leading to better performances.

## 5.4 Image Classification

Augmenting convolution models with self-attention (Bello et al., 2019; Parmar et al., 2019; Hu et al., 2019; Wang et al., 2019) provides the model with the ability to capture global contexts in an image and has yielded gains in several vision tasks such as image classification and object detection. We follow the protocols in (Bello et al., 2019), i.e. incorporating relative position embeddings for self-attention operations and augmenting each ResNet (Zagoruyko and Komodakis, 2016; He et al., 2016) block with self-attentions. To handle the prohibitive memory cost, (Bello et al., 2019) performs self-attention operations starting from the last layer, which has the smallest spatial dimension, until memory constraints are hit. This ad-hoc strategy is replaced by SAC.

	CIFAR-100					ImageNet			
	GFlops	top-1	top-5	Params		GFlops	top-1	top-5	Params
Wide-ResNet	10.4	80.3	95.0	36.3M	ResNet-50	8.2	76.4	93.1	25.6M
Bello et al. (2019)	10.9	81.6	95.2	36.2M		8.3	77.7	93.8	25.8M
SAC	11.0	<b>82.0</b>	<b>95.4</b>	36.2M		8.3	<b>78.3</b>	<b>94.2</b>	25.9M

Table 4: Results of image classification on CIFAR-100 using the Wide-ResNet 28-10 Zagoruyko and Komodakis (2016) as the backbone and on ImageNet using the ResNet-50 He et al. (2016) model.

Following (Bello et al., 2019), we conduct experiments on CIFAR-100 (Krizhevsky et al., 2009) and ImageNet (Deng et al., 2009). For CIFAR-100, we use the Wide-ResNet-28-10, the architecture of which comprises 3 stages of 4 residual blocks each using two  $3 \times 3$  convolutions. We augment each convolution of all residual blocks with the number of attention heads set to 16. For ImageNet, we use ResNet-50, the block of which consists of  $1 \times 1$ ,  $3 \times 3$ ,  $1 \times 1$  convolutions where the last pointwise convolution expands the number of filters and the first one contracts the number of filters. We tune  $\alpha$  in range  $\{5, 10, 20\}$ .

Results are shown in Table 4. As can be seen, the proposed SAC model significantly outperforms the attention model in (Bello et al., 2019) with the only modification of automatic edge construction. Specifically, the top-1 score increases from 81.6 to 82.0 for CIFAR-100 and from 77.7 to 78.3 for ImageNet. The improvement validates the importance of performing necessary attention operations under memory limit.

## 6 Conclusion and Future Work

In this work, we propose Sparse Adaptive Connection — a novel method to accelerate and structure the self-attention mechanism that adapts to various downstream tasks. We use an LSTM edge predictor to construct edges for self-attention operations, and introduce distance encodings to incorporate distance information into the learning process. In the future, we will consider applying this method to more tasks to verify its effectiveness. We are especially interested in how SAC can work in fully unsupervised tasks and learn inner structures of the data such as grammar induction. On the theoretical side, we will formalize SAC to show the relationships of existing self-attention methods.

## References

- Sami Abu-El-Haija, Bryan Perozzi, Rami Al-Rfou, and Alexander A Alemi. 2018. Watch your step: Learning node embeddings via graph attention. In S. Bengio, H. Wallach, H. Larochelle, K. Grauman, N. Cesa-Bianchi, and R. Garnett, editors, *Advances in Neural Information Processing Systems 31*, pages 9180–9190. Curran Associates, Inc.
- Rami Al-Rfou, Dokook Choe, Noah Constant, Mandy Guo, and Llion Jones. 2019. Character-level language modeling with deeper self-attention. In *Proceedings of the AAAI Conference on Artificial Intelligence*, volume 33, pages 3159–3166.
- Dzmitry Bahdanau, Kyunghyun Cho, and Yoshua Bengio. 2014. Neural machine translation by jointly learning to align and translate.
- Mikhail Belkin, Partha Niyogi, and Vikas Sindhwani. 2006. Manifold regularization: A geometric framework for learning from labeled and unlabeled examples. *J. Mach. Learn. Res.*, 7:2399–2434.
- Irwan Bello, Barret Zoph, Ashish Vaswani, Jonathon Shlens, and Quoc V. Le. 2019. Attention augmented convolutional networks. In *The IEEE International Conference on Computer Vision (ICCV)*.
- Danqi Chen and Christopher D Manning. 2014. A fast and accurate dependency parser using neural networks. In *Proceedings of the 2014 conference on empirical methods in natural language processing (EMNLP)*, pages 740–750.

- Rewon Child, Scott Gray, Alec Radford, and Ilya Sutskever. 2019. Generating long sequences with sparse transformers.
- Zihang Dai, Zhilin Yang, Yiming Yang, Jaime Carbonell, Quoc Le, and Ruslan Salakhutdinov. 2019. Transformer-XL: Attentive language models beyond a fixed-length context. In *Proceedings of the 57th Annual Meeting of the Association for Computational Linguistics*, pages 2978–2988, Florence, Italy. Association for Computational Linguistics.
- Michaël Defferrard, Xavier Bresson, and Pierre Vandergheynst. 2016. Convolutional neural networks on graphs with fast localized spectral filtering. In D. D. Lee, M. Sugiyama, U. V. Luxburg, I. Guyon, and R. Garnett, editors, *Advances in Neural Information Processing Systems 29*, pages 3844–3852. Curran Associates, Inc.
- Jia Deng, Wei Dong, Richard Socher, Li-Jia Li, Kai Li, and Li Fei-Fei. 2009. Imagenet: A large-scale hierarchical image database. In *2009 IEEE conference on computer vision and pattern recognition*, pages 248–255. Ieee.
- Qipeng Guo, Xipeng Qiu, Pengfei Liu, Yunfan Shao, Xiangyang Xue, and Zheng Zhang. 2019. Star-transformer. In *Proceedings of the 2019 Conference of the North American Chapter of the Association for Computational Linguistics: Human Language Technologies, Volume 1 (Long and Short Papers)*, pages 1315–1325, Minneapolis, Minnesota. Association for Computational Linguistics.
- Will Hamilton, Zhitao Ying, and Jure Leskovec. 2017a. Inductive representation learning on large graphs. In *Advances in neural information processing systems*, pages 1024–1034.
- Will Hamilton, Zhitao Ying, and Jure Leskovec. 2017b. Inductive representation learning on large graphs. In I. Guyon, U. V. Luxburg, S. Bengio, H. Wallach, R. Fergus, S. Vishwanathan, and R. Garnett, editors, *Advances in Neural Information Processing Systems 30*, pages 1024–1034. Curran Associates, Inc.
- William L. Hamilton, Rex Ying, and Jure Leskovec. 2017c. Representation learning on graphs: Methods and applications.
- Kaiming He, Xiangyu Zhang, Shaoqing Ren, and Jian Sun. 2016. Deep residual learning for image recognition. In *Proceedings of the IEEE conference on computer vision and pattern recognition*, pages 770–778.
- Sepp Hochreiter and Jürgen Schmidhuber. 1997. Long short-term memory. *Neural computation*, 9(8):1735–1780.
- Han Hu, Zheng Zhang, Zhenda Xie, and Stephen Lin. 2019. Local relation networks for image recognition. In *Proceedings of the IEEE International Conference on Computer Vision*, pages 3464–3473.
- Max Jaderberg, Karen Simonyan, Andrew Zisserman, and koray kavukcuoglu. 2015. Spatial transformer networks. In C. Cortes, N. D. Lawrence, D. D. Lee, M. Sugiyama, and R. Garnett, editors, *Advances in Neural Information Processing Systems 28*, pages 2017–2025. Curran Associates, Inc.
- Diederik P Kingma and Jimmy Ba. 2014. Adam: A method for stochastic optimization. *arXiv preprint arXiv:1412.6980*.
- Thomas N. Kipf and Max Welling. 2016. Semi-supervised classification with graph convolutional networks.
- Nikita Kitaev, Lukasz Kaiser, and Anselm Levskaya. 2020. Reformer: The efficient transformer. In *International Conference on Learning Representations*.
- Alex Krizhevsky, Geoffrey Hinton, et al. 2009. Learning multiple layers of features from tiny images.
- John Boaz Lee, Ryan Rossi, and Xiangnan Kong. 2018. Graph classification using structural attention. In *Proceedings of the 24th ACM SIGKDD International Conference on Knowledge Discovery & Data Mining*, page 1666–1674, New York, NY, USA. Association for Computing Machinery.

- Junhyun Lee, Inyeop Lee, and Jaewoo Kang. 2019. Self-attention graph pooling. In *Proceedings of the 36th International Conference on Machine Learning*, volume 97 of *Proceedings of Machine Learning Research*, pages 3734–3743, Long Beach, California, USA. PMLR.
- Renjie Liao, Zhizhen Zhao, Raquel Urtasun, and Richard Zemel. 2019. Lanczosnet: Multi-scale deep graph convolutional networks. In *International Conference on Learning Representations*.
- Arthur Liberzon, Aravind Subramanian, Reid Pinchback, Helga Thorvaldsdóttir, Pablo Tamayo, and Jill P Mesirov. 2011. Molecular signatures database (msigdb) 3.0. *Bioinformatics*, 27(12):1739–1740.
- Yanbin Liu, Juho Lee, Minseop Park, Saehoon Kim, Eunho Yang, Sung Ju Hwang, and Yi Yang. 2018. Learning to propagate labels: Transductive propagation network for few-shot learning. *arXiv preprint arXiv:1805.10002*.
- Qing Lu and Lise Getoor. 2003. Link-based classification. In *Machine Learning, Proceedings of the Twentieth International Conference (ICML 2003), August 21-24, 2003, Washington, DC, USA*, pages 496–503. AAAI Press.
- Matt Mahoney. 2011. Large text compression benchmark. URL: <http://www.matmahoney.net/text/text.html>.
- F. Monti, D. Boscaini, J. Masci, E. Rodola, J. Svoboda, and M. M. Bronstein. 2017. Geometric deep learning on graphs and manifolds using mixture model cnns. In *2017 IEEE Conference on Computer Vision and Pattern Recognition (CVPR)*, pages 5425–5434, Los Alamitos, CA, USA. IEEE Computer Society.
- Myle Ott, Sergey Edunov, David Grangier, and Michael Auli. 2018. Scaling neural machine translation. In *Proceedings of the Third Conference on Machine Translation: Research Papers*, pages 1–9, Brussels, Belgium. Association for Computational Linguistics.
- Niki Parmar, Prajit Ramachandran, Ashish Vaswani, Irwan Bello, Anselm Levskaya, and Jon Shlens. 2019. Stand-alone self-attention in vision models. In *Advances in Neural Information Processing Systems 32*, pages 68–80. Curran Associates, Inc.
- Hongbin Pei, Bingzhe Wei, Kevin Chen-Chuan Chang, Yu Lei, and Bo Yang. 2020. Geom-gcn: Geometric graph convolutional networks. In *International Conference on Learning Representations*.
- Bryan Perozzi, Rami Al-Rfou, and Steven Skiena. 2014. Deepwalk: Online learning of social representations. In *Proceedings of the 20th ACM SIGKDD International Conference on Knowledge Discovery and Data Mining, KDD '14*, page 701–710, New York, NY, USA. Association for Computing Machinery.
- Prithviraj Sen, Galileo Namata, Mustafa Bilgic, Lise Getoor, Brian Galligher, and Tina Eliassi-Rad. 2008. Collective classification in network data. *AI magazine*, 29(3):93–93.
- Rico Sennrich, Barry Haddow, and Alexandra Birch. 2016. Neural machine translation of rare words with subword units. In *Proceedings of the 54th Annual Meeting of the Association for Computational Linguistics (Volume 1: Long Papers)*, pages 1715–1725, Berlin, Germany. Association for Computational Linguistics.
- Sainbayar Sukhbaatar, Edouard Grave, Piotr Bojanowski, and Armand Joulin. 2019. Adaptive attention span in transformers. In *Proceedings of the 57th Annual Meeting of the Association for Computational Linguistics*, pages 331–335, Florence, Italy. Association for Computational Linguistics.
- C. Szegedy, V. Vanhoucke, S. Ioffe, J. Shlens, and Z. Wojna. 2016. Rethinking the inception architecture for computer vision. In *2016 IEEE Conference on Computer Vision and Pattern Recognition (CVPR)*, pages 2818–2826, Los Alamitos, CA, USA. IEEE Computer Society.
- Ashish Vaswani, Noam Shazeer, Niki Parmar, Jakob Uszkoreit, Llion Jones, Aidan N Gomez, Łukasz Kaiser, and Illia Polosukhin. 2017. Attention is all you need. In I. Guyon, U. V. Luxburg, S. Bengio, H. Wallach, R. Fergus, S. Vishwanathan, and R. Garnett, editors, *Advances in Neural Information Processing Systems 30*, pages 5998–6008. Curran Associates, Inc.

- Petar Veličković, Guillem Cucurull, Arantxa Casanova, Adriana Romero, Pietro Lio, and Yoshua Bengio. 2017. Graph attention networks. *arXiv preprint arXiv:1710.10903*.
- Petar Veličković, Guillem Cucurull, Arantxa Casanova, Adriana Romero, Pietro Liò, and Yoshua Bengio. 2018. Graph attention networks. In *International Conference on Learning Representations*.
- Petar Veličković, William Fedus, William L. Hamilton, Pietro Liò, Yoshua Bengio, and R Devon Hjelm. 2019. Deep graph infomax. In *International Conference on Learning Representations*.
- Hongwei Wang and Jure Leskovec. 2020. Unifying graph convolutional neural networks and label propagation. *arXiv preprint arXiv:2002.06755*.
- Qilong Wang, Banggu Wu, Pengfei Zhu, Peihua Li, Wangmeng Zuo, and Qinghua Hu. 2019. Eca-net: Efficient channel attention for deep convolutional neural networks. *arXiv preprint arXiv:1910.03151*.
- Xiaolong Wang, Ross Girshick, Abhinav Gupta, and Kaiming He. 2018. Non-local neural networks. In *The IEEE Conference on Computer Vision and Pattern Recognition (CVPR)*.
- Jason Weston, Frédéric Ratle, Hossein Mobahi, and Ronan Collobert. 2012. *Deep Learning via Semi-supervised Embedding*, pages 639–655. Springer Berlin Heidelberg, Berlin, Heidelberg.
- Ronald J Williams. 1992. Simple statistical gradient-following algorithms for connectionist reinforcement learning. *Machine learning*, 8(3-4):229–256.
- Felix Wu, Amauri Souza, Tianyi Zhang, Christopher Fifty, Tao Yu, and Kilian Weinberger. 2019. Simplifying graph convolutional networks. In *Proceedings of the 36th International Conference on Machine Learning*, volume 97 of *Proceedings of Machine Learning Research*, pages 6861–6871, Long Beach, California, USA. PMLR.
- Kelvin Xu, Jimmy Ba, Ryan Kiros, Kyunghyun Cho, Aaron Courville, Ruslan Salakhudinov, Rich Zemel, and Yoshua Bengio. 2015. Show, attend and tell: Neural image caption generation with visual attention. In *Proceedings of the 32nd International Conference on Machine Learning*, volume 37 of *Proceedings of Machine Learning Research*, pages 2048–2057, Lille, France. PMLR.
- Keyulu Xu, Chengtao Li, Yonglong Tian, Tomohiro Sonobe, Ken-ichi Kawarabayashi, and Stefanie Jegelka. 2018. Representation learning on graphs with jumping knowledge networks. *arXiv preprint arXiv:1806.03536*.
- Zhilin Yang, William Cohen, and Ruslan Salakhudinov. 2016a. Revisiting semi-supervised learning with graph embeddings. In *Proceedings of The 33rd International Conference on Machine Learning*, volume 48 of *Proceedings of Machine Learning Research*, pages 40–48, New York, New York, USA. PMLR.
- Zhilin Yang, William W Cohen, and Ruslan Salakhudinov. 2016b. Revisiting semi-supervised learning with graph embeddings. *arXiv preprint arXiv:1603.08861*.
- Yang Ye and Shihao Ji. 2019. Sparse graph attention networks.
- Ze Ye, Kin Sum Liu, Tengfei Ma, Jie Gao, and Chao Chen. 2020. Curvature graph network. In *International Conference on Learning Representations*.
- Zihao Ye, Qipeng Guo, Quan Gan, Xipeng Qiu, and Zheng Zhang. 2019. Bp-transformer: Modelling long-range context via binary partitioning.
- Sergey Zagoruyko and Nikos Komodakis. 2016. Wide residual networks. In *Proceedings of the British Machine Vision Conference (BMVC)*, pages 87.1–87.12. BMVA Press.
- Kai Zhang, Yaokang Zhu, Jun Wang, and Jie Zhang. 2020. Adaptive structural fingerprints for graph attention networks. In *International Conference on Learning Representations*.
- Xiaojin Zhu, Zoubin Ghahramani, and John Lafferty. 2003. Semi-supervised learning using gaussian fields and harmonic functions. In *Proceedings of the Twentieth International Conference on Machine Learning, ICML’03*, page 912–919. AAAI Press.
- Marinka Zitnik and Jure Leskovec. 2017. Predicting multicellular function through multi-layer tissue networks. *Bioinformatics*, 33(14):i190–i198.